

EPR and preparative studies of 5-*endo* cyclizations of radicals derived from alkenyl NHC-boranes bearing *tert*-butyl ester substituents

Wen Dai,[‡] Dennis P. Curran,^{*‡} and John C. Walton^{*†}

[‡] Department of Chemistry, University of Pittsburgh, Pittsburgh, Pennsylvania 15260, United States.

[†] EaStCHEM School of Chemistry, University of St. Andrews, St. Andrews, Fife, KY16 9ST, United Kingdom.

Abstract: Radical H-atom abstraction from a set of N-heterocyclic carbene (NHC) complexes of alkenylboranes bearing two *tert*-butyl ester substituents was studied by EPR spectroscopy. The initial boraallyl radical intermediates rapidly ring closed onto the O-atoms of their distal ester groups in 5-*endo* mode to yield 1,2-oxaborole radicals. Unexpectedly, two structural varieties of these radicals were identified from their EPR spectra. These proved to be two stable rotamers in which the carbonyl group of the *tert*-butyl ester was oriented towards and away from the NHC ring. These rotamers were akin to the *s-trans* and *s-cis* rotamers of α,β -unsaturated carbonyl compounds. Their stability was attributed to the *quasi-allylic* interaction of their unpaired electrons with the carbonyl units of their adjacent ester groups. EPR spectroscopic evidence for two rotamers of the analogous methyl ester containing NHC-oxaborole radicals was also obtained. An improved synthetic procedure for preparing rare NHC-boralactones was developed involving treatment of the alkenyl NHC-boranes with AIBN and *tert*-dodecanethiol.

INTRODUCTION

N-Heterocyclic carbene boryl radicals (hereafter NHC-boryl radicals) are emerging as important reactive intermediates with interesting structures.¹ Due to their relatively weak B–H bonds,² NHC-boranes participate as both reagents and reactants in various radical-mediated transformations including photopolymerizations.³

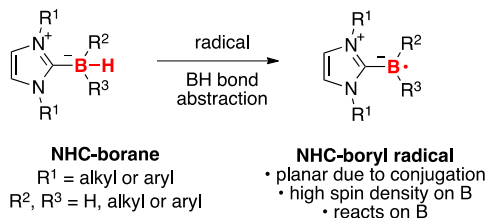
Structural knowledge about NHC-boryl radicals bearing assorted substituents on both the NHC ring and the boron atom comes from direct observation by EPR (Electron Paramagnetic Resonance; also known as Electron Spin Resonance) spectroscopy, often complemented by Density Functional Theory (DFT) calculations.⁴ NHC-boryl radicals are typically planar with spin density delocalized into the NHC ring due to conjugation (Figure 1a). Still, they are best considered as conjugated boryl radicals with carbon atoms in the π -system (as opposed to conjugated carbon radicals with a boron atom in the π -system) because they have relatively high spin density on boron and they typically react on boron.^{3,4}

Recently, we tried to make and observe boraallyl radicals **2** from NHC-alkenyl boranes **1** bearing two methyl ester substituents (Figure 1b).⁵ However, EPR experiments with **1** and *tert*-butyl peroxide (DTBP) provided spectra of a single species that did not match expectations for **2**. Instead, the observed spectra were assigned with the aid of DFT calculations to novel ring-closed 1,2-oxaborole radicals **3**.

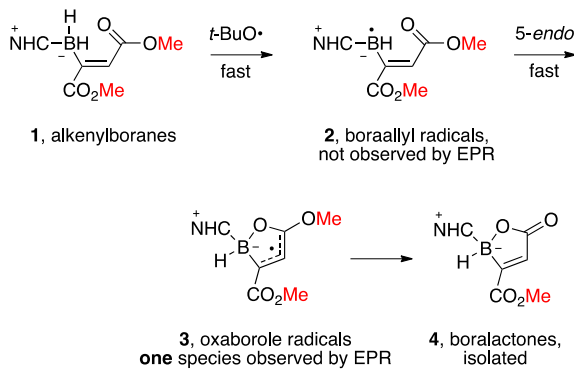
In complementary preparative experiments, reactions of **1** with AIBN and Bu₃SnH provided novel boralactones **4** as stable products in good yields. These boralactones are oxidized products, and oxygen (from air) is needed for their formation. Based on these results, we concluded that boraallyl radicals **2** were indeed generated under both EPR and preparative conditions, but they could not be observed by EPR because their *5-endo* cyclizations to 1,2-

oxaborole radicals **3** were so fast. This conclusion was supported by DFT calculations, which showed that the *5-endo* cyclization of **2** to **3** is both exothermic and has a low activation barrier.⁵

(a) Generation and generic structure of NHC-boryl radicals



(b) Unusual *5-endo* cyclizations of boraallyl radicals with methyl esters (ref. 5)



(c) EPR observation of two oxaborole radical species with *tert*-butyl esters (this work)

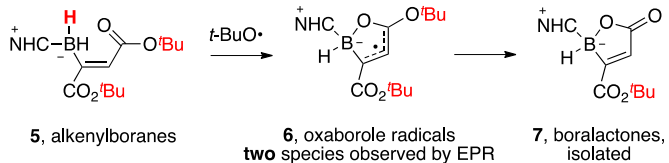


Figure 1. Structures and reactions of NHC-boryl radicals

As an extension of these studies, we decided to generate radicals from a set of analogous NHC-boranes **5** with di-*tert*-butyl ester groups (Figure 1c). This was conceived as a worthwhile if relatively routine extension of scope of the new cyclization to form oxaborole radicals. However, the EPR experiments held a surprise in store; we expected to observe one oxaborole radical species **6** on reactions of **5** with DTBP, but instead we observed two. Here we describe

these EPR experiments and associated DFT calculations and assign the two species as non-interconverting (on the EPR timescale at up to 300 K) rotamers of two oxaborole radicals. We also describe improved conditions based on thiol catalysis for preparative conversion of the various di-*tert*-butyl esters **6** to stable boralactones.

RESULTS AND DISCUSSION

Precursor Synthesis: The alkenylboranes **5a–f** used in this study are new compounds that were prepared by reaction of the parent NHC-boranes **8a–f** with di-*tert*-butyl acetylenedicarboxylate **9** (Scheme 1).⁶ Under a standard set of conditions, a mixture of the appropriate NHC-borane **8** (1 equiv) and **9** (2 equiv) in THF was refluxed for 12 h. Cooling, solvent removal, and direct purification by automated flash chromatography provided the alkenylborane **5** (less polar) along with the corresponding *trans*-borirane **10** (more polar). All the alkenyl boranes are pure (*E*)-isomers that are stable to ambient lab conditions.

Scheme 1. Synthesis of precursor alkenylboranes by hydroboration

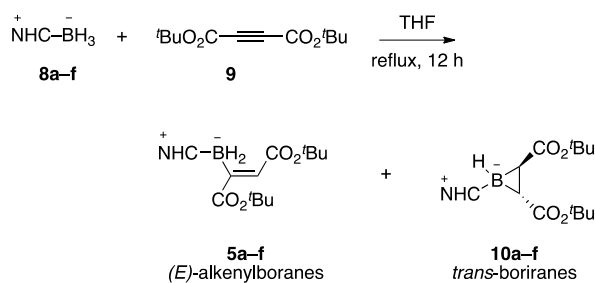
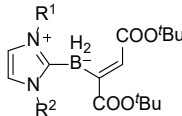
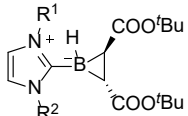
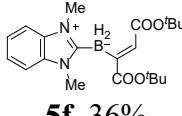
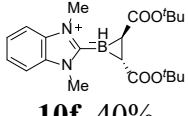


Table 1 summarizes the results of these preparative experiments. For the substrates with *N,N*-dialkyl substituents (entries 1–4 and 6), the ratio of alkenylborane **5** to borirane **10** was about 1/1. Isolated yields of the alkenylboranes **5a–d,f** were in the range of 36–44%, while total

isolated yields of both products (**5** + **10**) ranged from 75–83%. The exception was *N,N*-dimesityl substrate, entry 5. This reaction was conducted in acetonitrile, to aid precursor solubility, and provided mostly the borirane **10e** (53%) with only 15% of the alkenylborane **5e**. The increased amount of borirane in this experiment is due to the N-aryl substituents, not to the solvent change. Because of the small quantities available, **5e** was used only for EPR experiments.

Table 1. Isolated yields of alkenylboranes and boriranes.

| entry | alkenylborane, yield ^a | | borirane, yield ^a |
|---|---|------------------------------------|---|
| 1 |  | $R^1 = R^2 = \text{Me}$ |  |
| 2 | 5b , 42% | $R^1 = \text{Bu}, R^2 = \text{Me}$ | 10b , 41% |
| 3 | 5c , 39% | $R^1 = \text{Bn}, R^2 = \text{Me}$ | 10c , 36% |
| 4 | 5d , 40% | $R^1 = R^2 = i\text{Pr}$ | 10d , 37% |
| 5 ^b | 5e , 15% | $R^1 = R^2 = \text{Mes}$ | 10e , 53% |
| 6 |  | 5f , 36% |  |
| ^a isolated yield; ^b CH ₃ CN as solvent | | | |

EPR Spectroscopic Experiments: Solutions of each of the symmetrical NHC-alkenylboranes **5a**, **5d**, **5e** and **5f**, with added DTBP, were prepared in *tert*-butylbenzene solvent. Each solution was sonicated, then aliquots (0.2 mL) in quartz tubes were deaerated by bubbling N₂ and irradiated in the resonant cavity of the 9.5 GHz CW-EPR spectrometer with unfiltered UV light from a 500 W high pressure mercury arc lamp. Initially spectra were run at intervals in the temperature range 220 to 280 K with best results at about 260 K, except for **5e** for which the best quality signal was obtained at 220 K.

A spectrum with remarkable resolution was obtained in 2nd derivative mode from precursor alkenylborane **5a** at 270 K [see Figure 2(a)]. The spectrum of the major radical present consisted of a set of 8 doublets and was readily simulated with hyperfine splittings (hfs) of $a(1\text{H}) = 25.16$, $a(^{11}\text{B}) = 6.47$ and $a(1\text{H}) = 1.30$ G [see red spectrum (b) in Figure 2]. These hfs were of similar magnitude, where applicable, to those of the ring-closed oxaborole radical **3a** previously observed from the analogous precursor containing methyl ester substituents [$a(1\text{H}) = 26.01$, $a(^{11}\text{B}) = 6.01$, $a(1\text{H}) = 1.64$, $a(3\text{H}) = 1.12$ G].⁶ Hence the main species observed was the ring closed oxaborole radical **6a**. The simulation of the same radical with its ¹⁰B-isotope [Figure 2, green trace (c)] also conformed well with this conclusion.

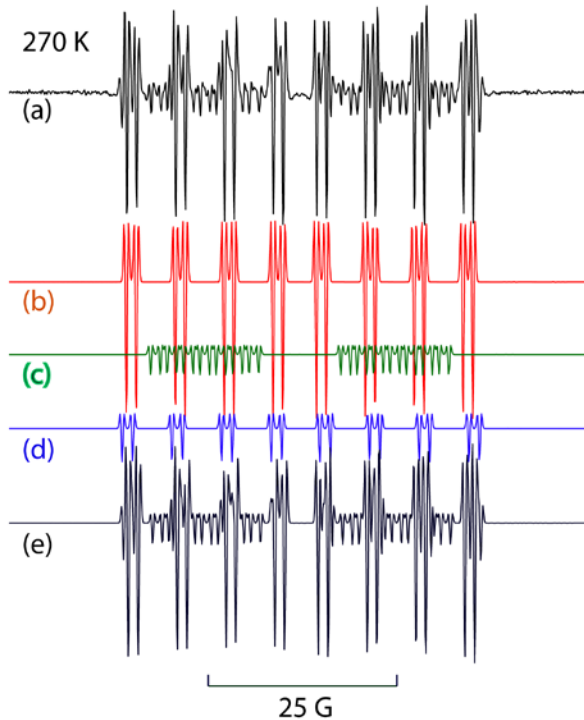
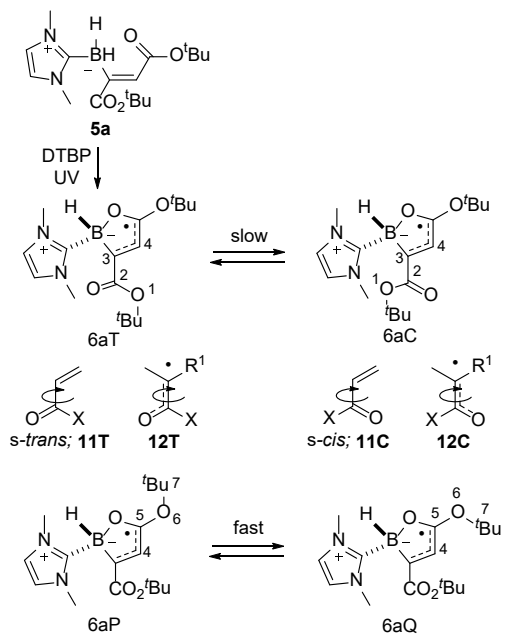


Figure 2. Experimental and simulated 2nd derivative CW EPR spectra obtained for ring-closed oxaborole radical **6a** from precursor **5a**. (a) Experimental spectrum at 270 K; (b) Simulation of major oxaborole rotamer of **6a** with ¹¹B isotope; (c) Simulation of major oxaborole rotamer of **6a**

with ^{10}B isotope; (d) Simulation of minor oxaborole rotamer of **6a** with ^{11}B isotope; (e) Sum (b + c + d) of simulations.

Surprisingly, the spectrum contained another minor radical (relative concentration 16%) with additional resonance lines most easily observed “outside”, that is to high and low field, of the main doublets. This spectrum was also effectively simulated as another set of 8 doublets [see blue trace (d) in Figure 2; the correlation coefficient for the sum of the simulations was $R = 0.983$]. The g -factor (2.0034) was essentially identical to that of the main species and the hfs [$a(1\text{H}) = 26.17$, $a(^{11}\text{B}) = 6.58$, $a(1\text{H}) = 1.38 \text{ G}$] were so similar as to suggest the major and minor species were structural varieties of the same ring-closed oxaborole radical **6a**.

The structural possibilities for oxaborole radical **6a** were investigated by means of DFT computations with the B3LYP functional and the 6-311+G(2d,p) basis set. In the lowest energy structure **6aT** (Scheme 2 and Figure 4) the C=O group was *trans* to the partial C=C double bond of the oxaborole ring and pointed approximately towards the NHC ring. Furthermore, the 5-member oxaborole ring, the ester CO₂ group and the O-atom of the lactone O'Bu group lay almost in a plane. The comparatively short bond from the ring C-atom to the ester carbonyl-C-atom [$r\text{C}^2-\text{C}^3$] in Scheme 2] i.e. 1.428 Å suggested some double bond character with consequent restricted rotation. The potential energy function for internal rotation of the CO₂'Bu group was obtained by successive incrementation of the dihedral angle 4-3-2-1 (see Scheme 2). Similarly, the rotational potential energy function for internal rotation of the O'Bu group (structures **6aP**, **6aQ**; dihedral angle 7-6-5-4) was also obtained and these energy profiles are illustrated in Figure 3.



Scheme 2. Conformational interconversions of 1,2-oxaborole radicals **6a**. Top: CO₂'Bu rotor; bottom: O'Bu rotor.

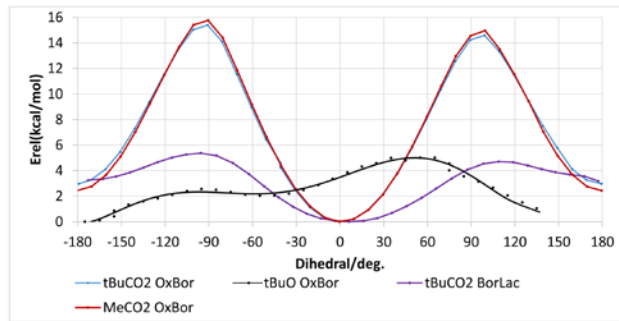


Figure 3. DFT potential energy functions for internal rotations in 1,2-oxaborole radicals **6a** and related species. Blue curve: torsional rotation of the CO₂'Bu group (dihedral angle 4-3-2-1) in **6a**. Red curve: torsional rotation of the CO₂Me group in **3a**. Black curve: rotation of the O'Bu group in **6a** (dihedral 4-5-6-7). Purple curve: torsional rotation of the CO₂'Bu group in boralactone **7a**.

The black curve (Figure 3) for torsion of the O'Bu group indicated only one stable conformation. Furthermore, the comparatively low computed energy barrier (~ 5 kcal/mol) suggested this motion would not be observable by EPR spectroscopy in the accessible temperature range. That is, the spectrum would be an average over all rotational states. On the other hand, the potential energy function for rotation of the $\text{CO}_2'\text{Bu}$ group was approximately that of a twofold rotor with just two stable rotamers (blue curve in Figure 3). The lowest energy rotamer, labelled **6aT** in Scheme 2 and Figure 4, had a dihedral angle 4-3-2-1 close to 0° such that the C=O of the ester group was *trans* to the adjacent ring C=C double bond and pointed towards the NHC ring. The second rotamer, labelled **6aC** in Scheme 2 and Figure 4, with its C=O group *cis* to the adjacent ring C=C double bond and pointing away from the NHC ring, had dihedral angle 4-3-2-1 close to 180° and was only 2.6 kcal/mol higher in energy.

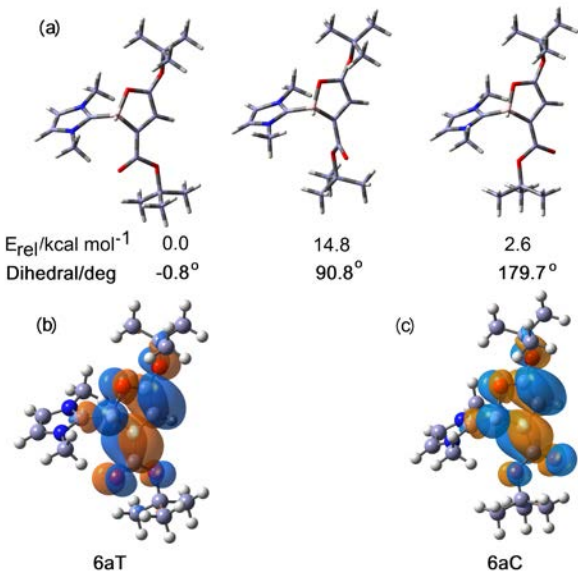
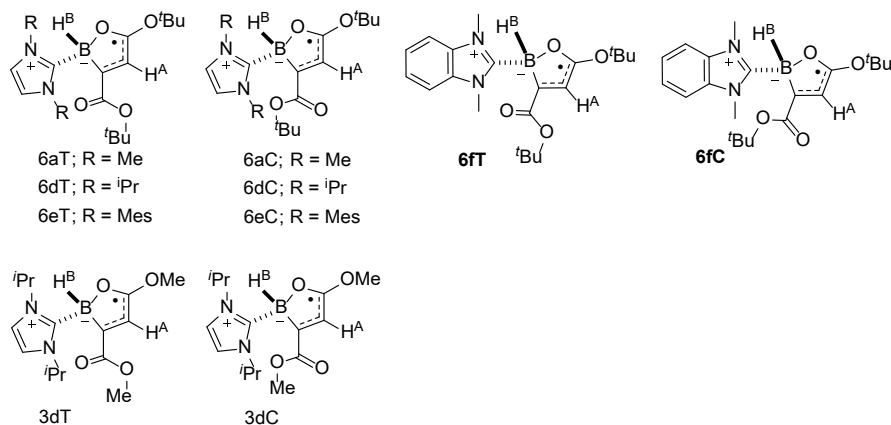


Figure 4. (a) DFT computed structures of internal rotation of the $\text{CO}_2'\text{Bu}$ group of oxaborole radical **6a**. Left; rotamer **6aT**, center; TS, right; rotamer **6aC**; (b) SOMO for **6aT**; (c) SOMO for **6aC**.

The HOMOs for the two stable rotamers are also illustrated in Figure 4. Interestingly, the HOMO for **6aT** consisted of an extensive π -system spanning the whole planar portion of the molecule including the ester C=O group (Figure 4 (b)). The second stable rotamer **6aC** contained an analogous planar region also covered by an extended π -system (Figure 4 (c)). The resonance electron delocalization resulting from these π -systems partly explains why these particular rotamers are energy minima. The comparatively high computed torsion barriers (15.4 and 14.6 kcal/mol) implied that interconversion of **6aT** and **6aC** would be very slow in the accessible temperature range. Consequently, these two rotamers should appear as separate species in the EPR spectrum. This DFT data enabled us to identify with some confidence **6aT** as the major radical present in the EPR spectrum and **6aC** as the minor radical.

Another conclusion from the DFT data is that CO₂'Bu groups in oxaborole radicals analogous to **6a**, but having different substituents on their NHC rings, should also have twofold torsional rotors. As predicted, the EPR spectra obtained from UV irradiation of solutions of **5d**, **5e** and **5f** each with DTBP did indeed demonstrate the presence of two rotamers of the corresponding oxaborole radicals. The spectra of **6d-f** were not so well resolved as in the case of radical **6a** but good simulations were achieved on inclusion of the second species. Sample spectra are included in the Supporting Information and the derived EPR parameters are in Table 2. The EPR results afforded good evidence that H-abstraction took place readily from precursors **5** and that the resulting boraallyl radicals (analogous to **2** but with 'Bu esters) ring closed very rapidly, even at 220 K, in *5-endo*-mode onto the O-atoms of the ester substituents.

Table 2. Experimental and computed EPR parameters for 1,2-oxaborole radicals **6** and **3**.^a



| Radical | T/K or DFT ^b | Rel. % | g-factor | <i>a</i> (¹¹ B) | <i>a</i> (¹⁰ B) | <i>a</i> (H ^B) | <i>a</i> (H ^A) | <i>a</i> (other) | R ^c |
|------------|-------------------------|--------|----------|-----------------------------|-----------------------------|----------------------------|----------------------------|----------------------|----------------|
| 6aT | 270 | 84 | 2.0034 | 6.47 | 2.17 | 25.16 | 1.30 | | 0.983 |
| 6aT | DFT | | | -6.06 | | 23.33 | -0.77 | | |
| 6aC | 270 | 16 | 2.0034 | 6.58 | | 26.17 | 1.39 | | 0.983 |
| 6aC | DFT | | | -6.21 | | 23.28 | -0.80 | | |
| 6dT | 260 | 79 | 2.0032 | 6.60 | 2.19 | 26.69 | 1.24 | | 0.988 |
| 6dC | 260 | 21 | 2.0032 | 6.65 | | 27.64 | 1.33 | | 0.988 |
| 6eT | 220 | 78 | 2.0037 | 6.50 | 2.15 | 24.64 | 1.20 | | 0.968 |
| 6eC | 220 | 22 | 2.0037 | 6.50 | | 25.54 | 1.25 | | 0.968 |
| 6fT | 260 | 79 | 2.0031 | 6.56 | 2.20 | 25.65 | 1.25 | | 0.962 |
| 6fC | 260 | 21 | 2.0031 | 6.65 | | 26.60 | 1.35 | | 0.962 |
| 3dT | 260 | 80 | 2.00340 | 6.63 | 2.21 | 26.76 | 1.64 | 1.03(3H) 0.61(3H) | 0.971 |
| 3aT | DFT ^d | | | -6.08 | - | 23.90 | -1.37 | 1.43(3H) 1.22(3H) | |
| 3dC | 260 | 20 | 2.00354 | 6.71 | - | 27.68 | 1.70 | 1.16(3H) 0.60(3H) | 0.971 |
| 3aC | DFT ^d | | | -6.18 | - | 23.81 | -1.25 | 1.45(3H) 1.18(3H) | |

^aHfs in Gauss (G); note that EPR provides only the magnitude not the sign of hfs. ^bDFT at the UB3LYP/6-311+G(2d,p) level of theory on oxaboroles with dimethyl-NHC units. ^cCorrelation coefficients of the computer simulations. ^dUB3LYP/epr-iii//UB3LYP/6-311+G(2d,p).

The spectra from radicals **6aT** and **6aC** were examined in the temperature range 220 to 280 K and showed the two distinct rotamers throughout. The ratio **6aT/6aC** was 84/16 at 270 K. It follows that interconversion of rotamer **6aT** with **6aC** was too slow for observation by EPR. Likewise, the spectra of radicals **6e–f** all showed two rotamers with T/C ratios of about 80/20. It is probable, therefore, that all the mixtures **6T** and **6C** were formed by hydrogen abstraction from corresponding conformations of the of the *E*-alkenylboranes **5**. In essence then, we can infer the rotamer ratios of precursors **5** (roughly 4/1 favoring *s-trans*) even though the rotation barriers in **5** are too low for direct measurement (for example, NMR spectra of **5** exhibit only a single set of signals). The assumption in this inference is that *tert*-butoxyl radicals react with the two rotamers of **5** at about the same rate.

The EPR spectra from all four precursors recorded at temperatures above about 300 K became more complex showing the presence of several radicals that could not be identified. These EPR spectra afforded no evidence of the formation of *tert*-butyl radicals from β -scission of 1,2-oxaborole radicals **6**. EPR spectra were also run on solutions of **5f** containing AIBN (2,2'-azobis(2-methylpropionitrile)) in place of DTBP. In the absence of UV irradiation, no EPR signals were detected at temperatures up to 350 K. When UV irradiation was introduced, the spectrum of the initiator-derived 2-cyanoprop-2-yl radical appeared. Prolonged heating with AIBN led to complex spectra but again no evidence for formation of *tert*-butyl radicals was obtained.

The two distinguishable rotamers of the set of ring-closed oxaborole radicals **6T** and **6C** resemble the *s-trans* and *s-cis* rotamers of α,β -unsaturated carbonyl compounds (Scheme 2, **11T** and **11C**), except that the ring C=C bonds of oxaborole radicals **6T** and **6C** have only partial double bond character. The barrier to internal rotation in acrolein (**11**, X = H) is only about 5

kcal/mol, as judged by ultrasonic⁷ and microwave spectroscopy measurements.⁸ Similarly, the barrier in acrylic acid (**11**, X = OH) was found experimentally to be 3.8 kcal/mol.⁹ Accordingly, conjugation of a carbonyl group with a C=C double bond creates a rotation barrier around a connecting single C–C bond of about 4–5 kcal/mol. However, the rotation barrier computed for oxaborole radicals **6aT** and **6aC** was calculated to be much higher at 14.6 kcal/mol, and a comparatively high value was supported by the EPR observation of distinct species. It follows that some other factor(s) must come into play.

For α -(alkoxycarbonyl)alkyl radicals **12T** and **12C** (X = OR) [and related species (X = alkyl, NR₂)] Fischer and co-workers observed two distinct rotamers by EPR spectroscopy.¹⁰ and also by muon spin resonance.¹¹ Newcomb and co-workers also adduced evidence for two conformational isomers for related ester radicals and showed that they reacted at different rates.¹² Furthermore, the energy barriers to internal rotation of these α -carbonylalkyl radicals were all determined to be in the range 10–12 kcal/mol.¹⁰⁻¹²

These structures and barrier heights show **12T** and **12C** to be better models for the oxaborole radicals. The comparatively large energy barriers to internal rotation, about what are formally single bonds in radicals **6**, can therefore be attributed to partial π -electron delocalization. The \bullet C–C=O units in oxaborole radicals **6** are partly allylic in character. More accurately the delocalization is *quasi*-pentadienylic because of the additional adjacent double bond in the oxaborole ring. The analogous internal rotation barrier \bullet C–C=C in the archetype allyl radical is somewhat higher at 15.7 kcal/mol¹³ as expected for full allylic character. The ratio of the s-*trans*-**6** to s-*cis*-**6** rotamers is close to 4:1 irrespective of the *N,N*-substituents on the NHC ring (see Table 2). Thus, steric hindrance from these substituents does not change the

rotamer populations and probably does not contribute much to the height of the ester internal rotation barriers either.

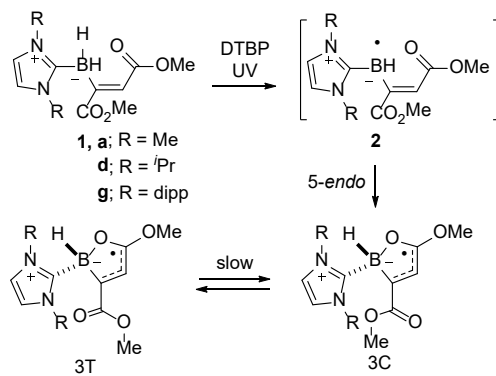
The torsion of the CO₂'Bu group in the isolated product boralactone **7a** was also examined by DFT computation. The potential energy function (purple curve in Figure 3) was similar in shape to that of the oxaborole radical showing an approximate twofold rotor with two stable conformations having their C=O groups *s-trans* and *s-cis* to the ring double bond and differing in energy by 3.2 kcal/mol. The computed barrier heights (4.7 and 5.4 kcal/mol) were considerably lower than for the oxaborole radicals because of the absence of the allylic type stabilization of the unpaired electron. As expected, these rotamers resemble those of α,β -unsaturated carbonyls **11T** and **11C**.

If these conclusions are correct, then it follows that distinct *s-trans* and *s-cis* rotamers would be expected for the analogous methyl ester containing oxaborole radicals **3** even though these were not detected in the original study.⁶ Internal rotation of the CO₂Me group in the dimethyl-NHC-oxaborole radical **3a** was therefore also examined by DFT computation. The computed potential energy function (red curve in Figure 3) revealed a twofold rotor very similar to that for analogous rotation of the CO₂'Bu group. Two stable rotamers **3aT** and **3aC** were indicated with their C=O groups in virtually the same orientations as in the CO₂'Bu analogs and differing in energy by only 2.4 kcal/mol. The rotational energy barriers (15.8 and 15.0 kcal/mol) were also similar and lent support to the idea that distinct rotamers should be observable for these species.

The previous EPR spectra of methyl ester containing oxaborole radicals **3** are considerably more complex than the new spectra of **6** because couplings to the methyl H-atoms of both the MeCO₂ and the MeO substituents are fully or partially resolved.⁶ These 1st

derivative EPR spectra gave no ostensible evidence for the presence of two rotamers. However, due to the intricate patterns of complex multiplets, minor proportions of a second rotamer could have gone undetected.

To look for the minor rotamer, a well resolved 2nd derivative spectrum for a methyl ester oxaborole radical **3** was needed (see Scheme 3). EPR spectra of the *N,N*-dimethyl-NHC-oxaborole radical **3a** were too weak and short-lived at all temperatures to permit recording in 2nd derivative mode. It is likely that the complexity and greater natural linewidth of the EPR spectrum of the *N,N*-di-dipp-NHC-oxaborole **3g** would obscure any minor rotamer even in a 2nd derivative spectrum.



Scheme 3. Generation of NHC-oxaborole radicals with methyl ester substituents.

We were, however, able to obtain a spectrum of the *N,N*-di-*i*Pr-NHC-oxaborole **3d** in 2nd derivative mode in a mixed solvent (Figure 5(a)).¹⁴ This spectrum revealed some asymmetry, and additional resonance lines were resolved. The simulation with just one rotamer of the methyl ester group (Figure 5(b)) had a correlation coefficient of 0.867, but a much-improved fit (R = 0.971) was achieved by inclusion of 19% of a second conformation (Figure 5(c)). The spectral asymmetry was attributable to a very slight difference in the g-factors of the two rotamers. See Table 2 for the resultant EPR parameters.

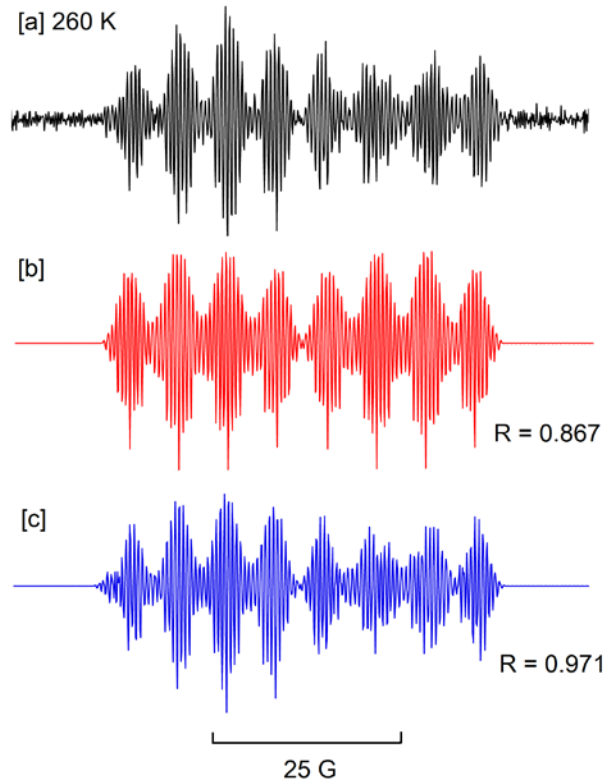


Figure 5. Experimental and simulated 2nd derivative CW EPR spectra obtained for ring-closed oxaborole radical **3d** from precursor **1d**. (a) Black: experimental spectrum at 260 K in Ph'Bu containing 5% allyl bromide. (b) Red: simulation of major oxaborole rotamer of **3dT** with ¹¹B and ¹⁰B isotopes. (c) Blue: simulation including major (**3dT**) and minor (**3dC**) rotamers of oxaborole radicals.

The detection of two rotamers of radical **3d** supports the idea that the internal rotation barriers arise from delocalization of the unpaired electron in the *quasi*-pentadieneylic π -systems. We conclude that two stable rotamers exist for RCO₂ substituents in other NHC-oxaborole radicals **3**, even though their signals cannot be resolved in their EPR spectra.

Preparative Reactions: To make boralactones, we initially used the conditions developed for the corresponding dimethyl esters as shown in Figure 6a.⁵ In this earlier work, alkenylboranes **1**

were heated in benzene (80 °C, 6 h) with AIBN (50 mol%) and Bu₃SnH (50 mol%) to provide NHC-boralactones **4** in isolated yields of about 60%. This procedure requires dioxygen for product formation, and preparative reactions are prone to stopping if the source is ambient air.

This published procedure worked reasonably well for the di-*tert*-butyl esters. For example, reaction of **5a** ($R^1 = R^2 = \text{Me}$) under these conditions provided **7a** in 44% yield according to ¹¹B NMR analysis of the crude product. However, substituting *tert*-dodecanethiol for tin hydride (Figure 6b) proved to be more practical because the products are free from tin.¹⁵ For example, reaction of **5a** under the thiol conditions provided **7a** in 70% yield according to ¹¹B NMR analysis. A control experiment quickly showed that this procedure does not require dioxygen, so the subsequent experiments were conducted under argon to discourage oxidation of the thiol to a disulfide.

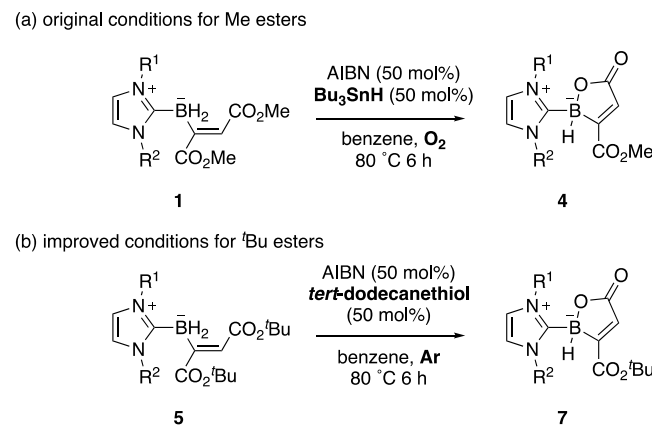


Figure 6. Conditions for boralactone formation

The structures and yields of the boralactones made by this procedure are shown in Figure 7. According to ¹¹B NMR analysis, the boralactones **7a–d** were formed in 64–70% yields. All

these boralactones are polar and purification by flash chromatography gave mixed results. Boralactones **7b**, **7d** and **7f** were isolated in good purity yields of 56%, 54% and 50%, respectively. Boralactone **7c** was isolated in 57% yield and was about 90% pure, while **7a** was isolated in 59% yield and was about 72% pure. The purities were determined by ^{11}B NMR spectroscopy, where the impurities show a very broad signal at about 0–5 ppm. This signal, which was present in the spectra of all the crude products, was completely removed for **7b**, **7d** and **7f**, partially removed for **7a**, and not removed for **7c**.

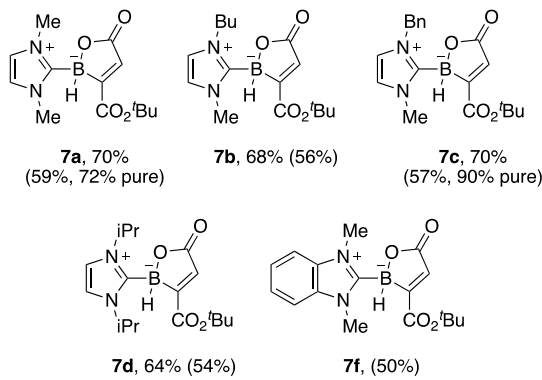


Figure 7. Structures and ^{11}B NMR yields of new boralactones (isolated yields are in parentheses).

Reaction Mechanism: Figure 8 shows a thiol-catalysis mechanism for boralactone formation that is consistent with the experimental results. Starting from boraalkenyl radical **11**, rapid (k probably $> 10^8 \text{ s}^{-1}$) 5-*endo* cyclization provides oxaborole radical **6**. This undergoes β -fragmentation to provide boralactone **7** and *tert*-butyl radical. This β -fragmentation does not occur when methyl is the departing radical,⁵ and even the liberation of the *tert*-butyl radical must be relatively slow (k probably $< 10^5 \text{ s}^{-1}$) because it is not observed by EPR spectroscopy (see

above). Based on prior work on thiol catalysis of NHC-borane reactions,^{3g,16} we suggest that the *tert*-butyl radical abstracts hydrogen from *tert*-dodecanethiol to give the corresponding thiyl-radical and *tert*-butane. In turn, the thiyl-radical abstracts hydrogen from the starting alkenylborane **5** to give back the thiol and the starting alkenylboryl radical **11**, thereby closing the chain cycle. This is a net redox-neutral reaction in which one product (the boralactone **7**) is oxidized relative to that starting alkenylborane **5** and the other (*tert*-butane) is reduced.

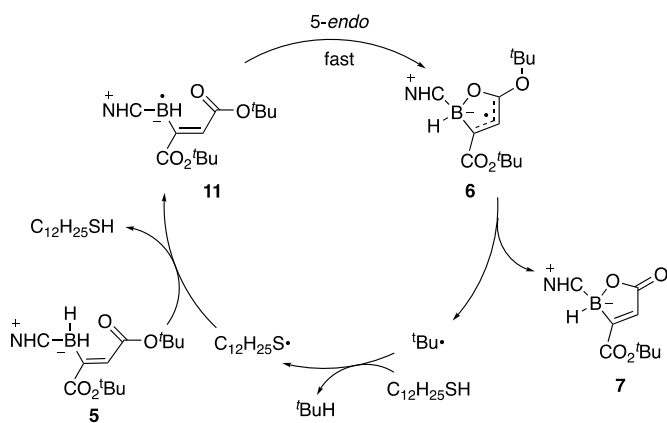


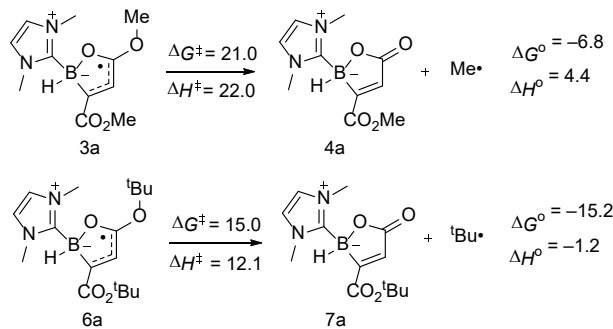
Figure 8. Putative thiol-catalysis mechanism for boralactone formation

To support the thiol catalysis mechanism, we conducted an experiment with **5d** under the standard conditions but reducing the amount of thiol from 50 mol% to 20 mol%. This provided **7d** in 68% NMR yield and 53% isolated yield (compare this to Figure 8, 64% NMR yield and 54% isolated yield of **7d** with 50 mol% thiol). Thus, a decrease in thiol amount by a factor of 2.5 does not materially affect the outcome of the reaction.

Support for the fragmentation of oxaborole radical **6a** to boralactone **7a** and *tert*-butyl radical was obtained from DFT computations. The transition state (TS) for extrusion of *tert*-

butyl radical from **6a** was located, and the resulting overall energetics and activation parameters are compared with those obtained previously⁶ for methyl radical extrusion from **3a** in Scheme 4 (see Supporting Information for details).

Scheme 4. DFT study of 1,2-oxaborole radical fragmentation. Method: B3LYP/6-311+G(2d,p); energies in kcal/mol



The fragmentation of **3a** was computed to be endothermic and both the activation enthalpy ($\Delta H^\ddagger = 22.0$ kcal mol⁻¹) and activation free energy ($\Delta G^\ddagger = 21.0$ kcal mol⁻¹) were too high for the elimination of methyl radical to be viable in solution. However, the fragmentation of **6a** to form *tert*-butyl radical was computed to be marginally exothermic ($\Delta H^0 = -1.2$ kcal/mol) and strongly exoergic ($\Delta G^0 = -15.2$ kcal/mol). Furthermore, both the activation enthalpy and free energy for loss of *tert*-butyl radical were low enough for the process to be viable at 80° C in solution ($\Delta H^\ddagger = 12.1$ kcal/mol; $\Delta G^\ddagger = 15.0$ kcal/mol). These DFT results support the mechanism proposed in Figure 8.

CONCLUSIONS

The straightforward hydroboration procedure with various NHC-BH₃ reagents succeeded as well with di-*tert*-butyl acetylenedicarboxylate as with the dimethyl-analogs. Most of the NHC-BH₃ reagents afforded readily separable mixtures of alkenyl NHC-boranes and boriranes in a ratio of about 1:1.

Hydrogen atom abstraction from *tert*-butyl ester-substituted NHC-alkenyl boranes by *tert*-butoxyl radicals was fast, generating boraallyl radicals **8**. The latter were not detectable by EPR spectroscopy even at 220 K but rapidly underwent an unusual *5-endo* ring closure onto the O-atom of the distal *tert*-butyl ester group. The EPR spectra showed the cyclization step to be fast at 220 K; as had previously been found for closure onto a methyl ester group. The allylic stabilization and extended π -conjugation of the oxaborole radicals undoubtedly contributed to the ease of these ring closure steps. Two distinct rotamers of each oxaborole radical were characterized by EPR spectroscopy and DFT computations. In these s-*trans* (**6T**) and s-*cis* (**6C**) rotamers the ester C=O groups adopted *trans* and *cis* orientations relative to the oxaborole ring C=C double bonds. The stability of these structures was due to the *quasi*-allylic interaction of the unpaired electron with the ester C=O group.

These observations implied that two stable rotamers of the analogous methyl ester substituted oxaborole radicals should also exist. Indeed, for one MeCO₂-containing oxaborole radical with a di-isopropyl-NHC unit, two distinct rotamers were spectroscopically characterized. It is likely that other MeCO₂-containing oxaborole radicals also exist as pairs of rotamers, but their EPR spectra are too complex for these to be distinguished with this spectroscopic technique. Newcomb and co-workers showed that the two analogous rotamers of appropriately unsaturated α -(alkoxycarbonyl)alkyl radicals reacted at different rates in subsequent cyclization steps.¹² It is therefore likely that the two rotamers of oxaborole radicals have different

reactivities particularly at C-3 (see Scheme 2). However, in our preparative processes (Figure 6) reaction took place at C-5 which is comparatively remote from the ester group. Differential reactivity at C-5 of the two ester conformations of oxaborole radicals will probably be insignificant.

The new preparative protocol for the boralactones, involving *tert*-dodecanethiol avoids the use of the neurotoxic tin hydride while also affording very acceptable yields. The products are examples of the rare NHC complexes of borinic acid lactones. They were found to be robust molecules with long shelf lives.

EXPERIMENTAL SECTION

Synthesis and Characterization of (*E*)-alkenylboranes and Boriranes

Di-*tert*-butyl but-2-ynedioate (di-*tert*-butyl acetylenedicarboxylate):¹⁷ *tert*-Butyl acetate (23.2 g, 200 mmol) and triflic acid (0.60 g, 4 mmol) were added dropwise to a solution of acetylenedicarboxylic acid (2.28 g, 20 mmol) in 150 mL of DCM at 0 °C. The resulting solution was warmed to room temperature with stirring for 2 h before saturated NaHCO₃ was slowly introduced. The aqueous layer was extracted with DCM (4 x 100 mL). The combined organic layer was washed with saturated NaCl, then dried over MgSO₄, filtered, and concentrated under reduced pressure to give crude product. This was purified by flash chromatography on silica (hexane:ethyl acetate) to afford the diester (3.16 g, 70%) as a colorless solid.

General hydroboration procedure: The NHC-borane (1 mmol) was added to a flask containing THF (10 mL), then di-*tert*-butyl acetylenedicarboxylate (0.45 g, 2 mmol) was added dropwise. The reaction mixture was heated at reflux. After 12 h, the mixture was concentrated,

and the resulting residue was purified by flash chromatography (hexane:ethyl acetate) to afford (*E*)-alkenylborane (less polar) followed by borirane (more polar).

(*E*)-(1,4-Di-*tert*-butoxy-1,4-dioxobut-2-en-2-yl)(1,3-dimethyl-1*H*-imidazol-3-ium-2-yl)dihydroborate (5a) and 2,3-bis(*tert*-butoxycarbonyl)-1-(1,3-dimethyl-1*H*-imidazol-3-ium-2-yl)boriran-1-uide (10a):

This experiment was conducted with **8a** (110 mg) and provided **5a** (148 mg, 44%, white solid, mp 79–81 °C) and **10a** (108 mg, 32%, yellow solid, mp 52–53 °C) after purification.

5a: ^1H NMR (500 MHz, CDCl_3) δ 6.77 (s, 2H), 6.23 (s, 1H), 3.70 (s, 6H), 1.39 (s, 9H), 1.33 (s, 9H); $^{13}\text{C}\{\text{H}\}$ NMR (125 MHz, CDCl_3) δ 174.7, 167.9, 127.6, 120.1, 79.3, 79.2, 36.1, 28.2, 28.1; ^{11}B NMR (160 MHz, CDCl_3) δ –28.8 (t, J = 88 Hz); HRMS (ESI, TOF) m/z [M – H] $^+$ calculated for $\text{C}_{17}\text{H}_{28}\text{BN}_2\text{O}_4$ 335.2142, found 335.2164.

10a: ^1H NMR (500 MHz, CDCl_3) δ 6.84 (s, 2H), 3.77 (s, 6H), 1.99 (dd, J = 8.1, 5.5 Hz, 1H), 1.82 (t, J = 4.8 Hz, 1H), 1.37 (s, 9H), 1.17 (s, 9H); $^{13}\text{C}\{\text{H}\}$ NMR (125 MHz, CDCl_3) δ 177.2, 176.9, 120.7, 77.4, 77.1, 36.0, 28.5, 28.2; ^{11}B NMR (160 MHz, CDCl_3) δ –27.0 (d, J = 123 Hz); HRMS (ESI, TOF) m/z [M + H] $^+$ calculated for $\text{C}_{17}\text{H}_{30}\text{BN}_2\text{O}_4$ 337.2299, found 337.2321.

(*E*)-(3-Butyl-1-methyl-1*H*-imidazol-3-ium-2-yl)(1,4-di-*tert*-butoxy-1,4-dioxobut-2-en-2-yl)dihydroborate (5b) and 2,3-bis(*tert*-butoxycarbonyl)-1-(3-butyl-1-methyl-1*H*-imidazol-3-ium-2-yl)boriran-1-uide (10b): This experiment was conducted with **8b** (152 mg) and provided

5b (160 mg, 42%, colorless oil) and **10b** (157 mg, 41%, colorless oil) after purification.

5b: ^1H NMR (500 MHz, CDCl_3) δ 6.80 (d, J = 1.9 Hz, 1H), 6.78 (d, J = 1.9 Hz, 1H), 6.26 (s, 1H), 4.13–4.04 (m, 2H), 3.73 (s, 3H), 1.71 (m, 2H), 1.42 (s, 9H), 1.35 (s, 9H), 0.92 (t, J = 7.4 Hz, 3H); $^{13}\text{C}\{\text{H}\}$ NMR (125 MHz, CDCl_3) δ 174.6, 167.9, 127.7, 120.2, 118.5, 79.2, 79.1, 48.5,

36.1, 32.4, 28.2, 28.1, 19.8, 13.7; ^{11}B NMR (160 MHz, CDCl_3) δ -28.8 (t, J = 88 Hz); HRMS (ESI, TOF) m/z [M - H] $^+$ calculated for $\text{C}_{20}\text{H}_{34}\text{BN}_2\text{O}_4$ 377.2612, found 377.2628.

10b: ^1H NMR (500 MHz, CDCl_3) δ 6.84 (d, J = 8.2 Hz, 2H), 4.22 (m, 2H), 3.83 (s, 3H), 2.06 (dd, J = 8.2, 5.5 Hz, 1H), 1.86 (t, J = 4.9 Hz, 1H), 1.81 (m, 2H), 1.43 (s, 9H), 1.24 (s, 9H), 0.97 (t, J = 7.4 Hz, 3H); $^{13}\text{C}\{\text{H}\}$ NMR (125 MHz, CDCl_3) δ 177.3, 177.1, 120.5, 119.3, 77.5, 77.2, 48.8, 36.1, 32.3, 28.5, 28.3, 19.7, 13.6; ^{11}B NMR (160 MHz, CDCl_3) δ -26.9 (d, J = 123 Hz); HRMS (ESI, TOF) m/z [M + H] $^+$ calculated for $\text{C}_{20}\text{H}_{36}\text{BN}_2\text{O}_4$ 379.2768, found 379.2786.

(E)-(3-Benzyl-1-methyl-1*H*-imidazol-3-ium-2-yl)(1,4-di-*tert*-butoxy-1,4-dioxobut-2-en-2-yl)dihydroborate (5c) and 1-(3-benzyl-1-methyl-1*H*-imidazol-3-ium-2-yl)-2,3-bis(*tert*-butoxycarbonyl)boriran-1-uide (10c): This experiment was conducted with **8c** (186 mg) and provided **5c** (161 mg, 39%, yellow solid) and **10c** (148 mg, 36%, yellow solid, mp 66–68 °C) after purification.

5c: ^1H NMR (500 MHz, CDCl_3) δ 7.27–7.19 (m, 5H), 6.69 (d, J = 2.0 Hz, 1H), 6.56 (d, J = 2.0 Hz, 1H), 6.22 (s, 1H), 5.27 (s, 2H), 3.72 (s, 3H), 1.34 (s, 9H), 1.32 (s, 9H); $^{13}\text{C}\{\text{H}\}$ NMR (125 MHz, CDCl_3) δ 167.9, 135.9, 128.8, 128.6, 128.2, 127.9, 120.5, 118.5, 79.3, 77.2, 52.2, 36.2, 28.2, 28.1; ^{11}B NMR (160 MHz, CD_3CN) δ -28.6 (t, J = 88 Hz); HRMS (ESI, TOF) m/z [M - H] $^+$ calculated for $\text{C}_{23}\text{H}_{32}\text{BN}_2\text{O}_4$ 411.2455, found 411.2473.

10c: ^1H NMR (500 MHz, CDCl_3) δ 7.35 (s, 5H), 6.82 (d, J = 2.0 Hz, 1H), 6.76 (d, J = 1.9 Hz, 1H), 5.46 (d, J = 14.7 Hz, 1H), 5.36 (d, J = 14.7 Hz, 1H), 3.86 (s, 3H), 2.13 (dd, J = 8.1, 5.5 Hz, 1H), 1.94 (t, J = 4.9 Hz, 1H), 1.42 (s, 9H), 1.29 (s, 9H); $^{13}\text{C}\{\text{H}\}$ NMR (125 MHz, CDCl_3) δ 177.2, 129.0, 128.6, 128.6, 120.9, 119.2, 77.6, 77.4, 52.5, 36.2, 28.5, 28.3, 28.2; ^{11}B NMR (160 MHz, CDCl_3) δ -26.9 (d, J = 123 Hz); HRMS (ESI, TOF) m/z [M + H] $^+$ calculated for $\text{C}_{23}\text{H}_{34}\text{BN}_2\text{O}_4$ 413.2612, found 413.2629.

(E)-(1,4-Di-*tert*-butoxy-1,4-dioxobut-2-en-2-yl)(1,3-diisopropyl-1*H*-imidazol-3-ium-2-yl)dihydroborate (5d) and 2,3-bis(*tert*-butoxycarbonyl)-1-(1,3-diisopropyl-1*H*-imidazol-3-ium-2-yl)boriran-1-uide (10d): This experiment was conducted with **8d** (166 mg) and provided **5d** (157 mg, 40%, white solid, mp 98–100 °C) and **10d** (145 mg, 37%, white solid, mp 103–105 °C) after purification.

5d: ^1H NMR (500 MHz, CDCl_3) δ 6.91 (s, 2H), 6.18 (s, 1H), 5.15 (hept, J = 6.8 Hz, 2H), 1.40 (s, 9H), 1.39 (s, 9H), 1.37 (s, 6H), 1.36 (s, 6H); $^{13}\text{C}\{\text{H}\}$ NMR (125 MHz, CDCl_3) δ 174.8, 167.6, 126.4, 115.0, 79.0, 49.2, 28.2, 28.2, 22.9; ^{11}B NMR (160 MHz, CDCl_3) δ –28.8 (t, J = 88 Hz); HRMS (ESI, TOF) m/z [M – H] $^+$ calculated for $\text{C}_{21}\text{H}_{36}\text{BN}_2\text{O}_4$ 391.2768, found 391.2787.

10d: ^1H NMR (500 MHz, CDCl_3) δ 6.96 (s, 2H), 5.33–5.19 (m, 2H), 2.02 (dd, J = 7.9, 5.4 Hz, 1H), 1.86 (t, J = 5.0 Hz, 1H), 1.43 (m, 21H), 1.31–1.23 (m, 9H); $^{13}\text{C}\{\text{H}\}$ NMR (125 MHz, CDCl_3) δ 177.5, 177.3, 115.7, 115.6, 77.4, 49.8, 28.6, 28.5, 28.0, 23.3, 22.8; ^{11}B NMR (160 MHz, CDCl_3) δ –26.9 (d, J = 121 Hz); HRMS (ESI, TOF) m/z [M + H] $^+$ calculated for $\text{C}_{21}\text{H}_{38}\text{BN}_2\text{O}_4$ 393.2925, found 393.2942.

(E)-(1,4-Di-*tert*-butoxy-1,4-dioxobut-2-en-2-yl)(1,3-dimesityl-1*H*-imidazol-3-ium-2-yl)dihydroborate (5e) and 2,3-bis(*tert*-butoxycarbonyl)-1-(1,3-dimesityl-1*H*-imidazol-3-ium-2-yl)boriran-1-uide (10e): This experiment was conducted with **8e** (318 mg) and provided **5e** (82 mg, 15%, white solid) and **10e** (289 mg, 53%, white solid) after purification.

5e: ^1H NMR (500 MHz, CDCl_3) δ 6.91 (s, 4H), 6.89 (s, 2H), 6.07 (s, 1H), 2.31 (s, 6H), 2.15 (s, 12H), 1.37 (s, 9H), 1.30 (s, 9H); $^{13}\text{C}\{\text{H}\}$ NMR (125 MHz, CDCl_3) δ 172.3, 138.6, 135.5, 134.4, 130.9, 120.0, 120.8, 78.4, 78.1, 77.2, 28.3, 28.1, 21.1, 18.1; ^{11}B NMR (160 MHz, CDCl_3) δ –28.3 (t, J = 91 Hz); HRMS (ESI, TOF) m/z [M – H] $^+$ calculated for $\text{C}_{33}\text{H}_{44}\text{BN}_2\text{O}_4$ 543.3394, found 543.3402.

10e: ^1H NMR (500 MHz, CDCl_3) δ 7.01 (s, 2H), 7.00 (s, 2H), 6.96 (s, 2H), 2.36 (s, 6H), 2.18 (s, 6H), 2.12 (s, 6H), 1.57 (dd, $J = 8.7, 6.5$ Hz, 1H), 1.31 (s, 9H), 1.29 (s, 9H), 1.13–1.08 (m, 1H); $^{13}\text{C}\{\text{H}\}$ NMR (125 MHz, CDCl_3) δ 178.2, 176.9, 139.1, 135.1, 135.0, 134.0, 129.5, 129.3, 122.0, 28.6, 28.5, 21.1, 18.3, 18.2; ^{11}B NMR (160 MHz, CDCl_3) δ –26.0 (d, $J = 122$ Hz); HRMS (ESI, TOF) m/z [M + H] $^+$ calculated for $\text{C}_{33}\text{H}_{46}\text{BN}_2\text{O}_4$ 545.3550, found 545.3557.

(E)-(1,4-Di-*tert*-butoxy-1,4-dioxobut-2-en-2-yl)(1,3-dimethyl-1*H*-benzo[d]imidazol-3-ium-2-yl)dihydroborate (5f) and 2,3-bis(*tert*-butoxycarbonyl)-1-(1,3-dimethyl-1*H*-benzo[d]imidazol-3-ium-2-yl)boriran-1-uide (10f): This experiment was conducted with **8f** (160 mg) and provided **5f** (139 mg, 36%, yellow solid, mp 100–101 °C) and **10f** (155 mg, 40%, yellow solid, mp 170–172 °C) after purification.

5f: ^1H NMR (500 MHz, CDCl_3) δ 7.46–7.41 (m, 2H), 7.38 (m, 2H), 6.35 (s, 1H), 3.95 (s, 6H), 1.32 (s, 9H), 1.31 (s, 9H); $^{13}\text{C}\{\text{H}\}$ NMR (125 MHz, CDCl_3) δ 174.4, 167.8, 133.2, 128.2, 123.9, 110.7, 79.4, 32.3, 28.1, 28.0; ^{11}B NMR (160 MHz, CDCl_3) δ –28.4 (t, $J = 89$ Hz); HRMS (ESI, TOF) m/z [M – H] $^+$ calculated for $\text{C}_{21}\text{H}_{30}\text{BN}_2\text{O}_4$ 385.2299, found 385.2317.

10f: ^1H NMR (500 MHz, CDCl_3) δ 7.50–7.39 (m, 4H), 4.04 (s, 6H), 2.19 (dd, $J = 8.3, 5.4$ Hz, 1H), 1.97 (t, $J = 5.0$ Hz, 1H), 1.46 (s, 9H), 1.11 (s, 9H); $^{13}\text{C}\{\text{H}\}$ NMR (125 MHz, CDCl_3) δ 177.0, 176.8, 132.8, 124.8, 121.2, 111.0, 107.3, 77.7, 77.3, 32.5, 28.5, 28.1, 26.0; ^{11}B NMR (160 MHz, CDCl_3) δ –26.9 (d, $J = 123$ Hz); HRMS (ESI, TOF) m/z [M + H] $^+$ calculated for $\text{C}_{21}\text{H}_{32}\text{BN}_2\text{O}_4$ 387.2455, found 387.2474.

DFT Calculations

DFT calculations were carried out using the Gaussian 09 suite of programs. Results were obtained with the B3LYP functional and the 6-311+G(2d,p) basis set was employed with the

CPCM continuum model with toluene as solvent. Default values of the keywords Alpha, Radii, TSNUM, and TSARE were employed. Vibrational frequency calculations were implemented so that GS (no imaginary frequencies) and TS status could be checked (one imaginary frequency), and enthalpies and free energies were adjusted for zero point and thermal corrections to 1 atm and 298 K.

EPR Experiments

CW-EPR spectra were obtained at 9.5 GHz with 100 kHz modulation employing a commercial spectrometer fitted with a rectangular ER4122 SP resonant cavity. Stock solutions of each sample (2 to 15 mg) and DTBP (1 equiv. wt/wt) in solvent (0.5 mL) were prepared and sonicated if necessary. An aliquot (0.2 mL), to which any additional reactant had been added, was placed in a 4 mm o. d. quartz tube and de-aerated by bubbling nitrogen for 15 min. Photolysis in the resonant cavity was by unfiltered light from a 500 W super pressure mercury arc lamp. In all cases where spectra were obtained, hfs were assigned with the aid of computer simulations using the Bruker SimFonia and NIEHS Winsim2002 software packages. EPR signals were digitally filtered and double integrated using the Bruker WinEPR software. The majority of EPR spectra were recorded with 2.0 mW power, 0.8 G_{pp} modulation intensity and a gain of ca. 10⁶.

Synthesis and Characterization of Boralactones

General Procedure: The (*E*)-alkenyl borane (0.1 mmol), benzene (1 mL), AIBN (8.2 mg, 0.05 mmol) and *tert*-dodecanethiol (10.1 mg, 0.05 mmol) were mixed and placed in a round bottomed flask with stir bar. The mixture was stirred at 80 °C under argon. After 6 h the reaction mixture

was concentrated under reduced pressure. The crude residue was purified by flash chromatography to afford the boralactone.

3-(*tert*-Butoxycarbonyl)-2-(3-butyl-1-methyl-1*H*-imidazol-3-ium-2-yl)-5-oxo-2,5-dihydro-

1,2-oxaborol-2-uide (7b): This experiment was conducted with **5a** (37.8 mg) and provided **7b** (18.0 mg, 56%, colorless oil) after purification. ^1H NMR (400 MHz, CDCl_3) δ 6.92 (d, J = 7.8 Hz, 2H), 6.61 (d, J = 2.0 Hz, 1H), 4.16 (ddd, J = 13.7, 8.5, 6.8 Hz, 1H), 3.96 (ddd, J = 13.7, 8.4, 6.6 Hz, 1H), 3.73 (s, 3H), 1.79 – 1.69 (m, 2H), 1.41 (s, 9H), 1.38–1.25 (m, 2H), 0.92 (t, J = 7.4 Hz, 3H); $^{13}\text{C}\{\text{H}\}$ NMR (101 MHz, CDCl_3) δ 176.2, 166.5, 132.0, 121.2, 119.4, 79.3, 47.9, 35.2, 31.8, 27.1, 18.7, 12.6; ^{11}B NMR (128 MHz, CDCl_3) δ –5.9 (d, J = 107 Hz); HRMS (ESI, TOF) m/z [M + H] $^+$ calculated for $\text{C}_{16}\text{H}_{26}\text{BN}_2\text{O}_4$ 321.1980, found 321.1999.

3-(*tert*-Butoxycarbonyl)-2-(1,3-diisopropyl-1*H*-imidazol-3-ium-2-yl)-5-oxo-2,5-dihydro-1,2-oxaborol-2-uide (7d):

This experiment was conducted with **5d** (39.2 mg) and provided **7d** (18.0 mg, 54%, colorless oil) after purification. ^1H NMR (400 MHz, CDCl_3) δ 7.09 (s, 2H), 6.58 (d, J = 2.0 Hz, 1H), 4.87 (hept, J = 6.7 Hz, 2H), 1.44 (d, J = 6.7 Hz, 6H), 1.40 (s, 9H), 1.38 (d, J = 6.7 Hz, 6H); $^{13}\text{C}\{\text{H}\}$ NMR (101 MHz, CDCl_3) δ 177.2, 167.6, 132.5, 116.9, 80.3, 49.9, 28.1, 23.4, 23.2; ^{11}B NMR (128 MHz, CDCl_3) δ –6.1 (broad); HRMS (ESI, TOF) m/z [M + H] $^+$ calculated for $\text{C}_{17}\text{H}_{28}\text{BN}_2\text{O}_4$ 335.2136, found 335.2148.

3-(*tert*-Butoxycarbonyl)-2-(1,3-dimethyl-1*H*-benzo[*d*]imidazol-3-ium-2-yl)-5-oxo-2,5-

dihydro-1,2-oxaborol-2-uide (7f): This experiment was conducted with **5f** (38.6 mg) and provided **7f** (16.4 mg, 50%, pale yellow oil) after purification. ^1H NMR (500 MHz, CDCl_3) δ 7.56–7.52 (m, 2H), 7.50 (m, 2H), 6.67 (d, J = 2.1 Hz, 1H), 3.96 (s, 6H), 1.39 (s, 9H); $^{13}\text{C}\{\text{H}\}$ NMR (125 MHz, CDCl_3) δ 177.3, 167.3, 133.5, 133.2, 125.3, 111.4, 80.5, 32.3, 28.1; ^{11}B NMR

(160 MHz, CDCl_3) δ -5.4 (d, $J = 108$ Hz); HRMS (ESI, TOF) m/z $[\text{M}+\text{H}]^+$ calculated for $\text{C}_{17}\text{H}_{22}\text{BN}_2\text{O}_4$ 329.1673, found 329.1687.

ASSOCIATED CONTENT

Supporting Information. Contains details of EPR experiments and calculations with copies of spectra of all compounds. This material is available free of charge via the Internet at <http://pubs.acs.org>.

AUTHOR INFORMATION

Corresponding Authors

* jcw@st-andrews.ac.uk; * curran@pitt.edu

ORCID

Wen Dai: 0000-0002-9098-5215

Dennis P. Curran: 0000-0001-9644-7728

John C. Walton: 0000-0003-2746-6276

ACKNOWLEDGMENTS

J.C.W. thanks EaStCHEM for financial support and D.P.C. thanks the US National Science Foundation. Computational support was provided through the EaStCHEM Research Computing Facility.

References and Notes

1. Ueng, S.-H.; Makhlof Brahmi, M.; Derat, É.; Fensterbank, L.; Lacôte, E.; Malacria, M.; Curran, D. P., Complexes of Borane and N-Heterocyclic Carbenes: A New Class of Radical Hydrogen Atom Donor. *J. Am. Chem. Soc.* **2008**, *130*, 10082-10083.
2. (a) Hioe, J.; Karton, A.; Martin, J. M. L.; Zipse, H., Borane-Lewis Base Complexes as Homolytic Hydrogen Atom Donors. *Chem. Eur. J.* **2010**, *16*, 6861-6865; (b) Tehfe, M.-A.; Monot, J.; Makhlof Brahmi, M.; Bonin-Dubarle, H.; Curran, D. P.; Malacria, M.; Fensterbank, L.; Lacôte, E.; Lalevée, J.; Fouassier, J.-P., N-Heterocyclic Carbene-Borane Radicals as Efficient Initiating Species of Photopolymerization Reactions under Air. *Polym. Chem.* **2011**, *2*, 625-631; (c) Tehfe, M.-A.; Makhlof Brahmi, M.; Fouassier, J.-P.; Curran, D. P.; Malacria, M.; Fensterbank, L.; Lacôte, E.; Lalevée, J., N-Heterocyclic Carbene Borane Complexes: A New Class of Initiators for Radical Photopolymerization. *Macromolecules* **2010**, *43*, 2261-2267.
3. (a) Shimoji, M.; Watanabe, T.; Maeda, K.; Curran Dennis, P.; Taniguchi, T., Radical *trans*-Hydroboration of Alkynes with N-Heterocyclic Carbene Boranes. *Angew. Chem. Int. Ed.* **2018**, *57*, 9485-9490; (b) Watanabe, T.; Hirose, D.; Curran, D. P.; Taniguchi, T., Borylative Radical Cyclizations of Benzo[3,4]Cyclodec-3-Ene-1,5-Diynes and N-Heterocyclic Carbene-Boranes. *Chem. Eur. J.* **2017**, *23*, 5404-5409; (c) Ren, S.-C.; Zhang, F.-L.; Qi, J.; Huang, Y.-S.; Xu, A.-Q.; Yan, H.-Y.; Wang, Y.-F., Radical Borylation/Cyclization Cascade of 1,6-Enynes for the Synthesis of Boron-Handled Hetero- and Carbocycles. *J. Am. Chem. Soc.* **2017**, *139*, 6050-6053; (d) Tambutet, G.; Guindon, Y., Diastereoselective Radical Hydrogen Transfer Reactions Using N-Heterocyclic Carbene Boranes. *J. Org. Chem.* **2016**, *81*, 11427-11431; (e) Kawamoto, T.; Geib, S. J.; Curran, D. P., Radical Reactions of N-Heterocyclic Carbene Boranes with Organic Nitriles: Cyanation of NHC-Boranes and Reductive Decyanation of Malononitriles. *J. Am. Chem. Soc.* **2015**, *137*, 8617-8622; (f) Kawamoto, T.; Okada, T.; Curran, D. P.; Ryu, I.,

Efficient Hydroxymethylation Reactions of Iodoarenes Using Co and 1,3-Dimethylimidazol-2-ylidene Borane. *Org. Lett.* **2013**, *15*, 2144-2147; (g) Pan, X.; Lacôte, E.; Lalevée, J.; Curran, D. P., Polarity Reversal Catalysis in Radical Reductions of Halides by N-Heterocyclic Carbene Boranes. *J. Am. Chem. Soc.* **2012**, *134*, 5669-5675; (h) Ueng, S.-H.; Fensterbank, L.; Lacôte, E.; Malacria, M.; Curran, D. P., Radical Deoxygenation of Xanthates and Related Functional Groups with New Minimalist N-Heterocyclic Carbene Boranes. *Org. Lett.* **2010**, *12*, 3002-3005.

4. (a) Walton, J. C.; Brahmi, M. M.; Monot, J.; Fensterbank, L.; Malacria, M.; Curran, D. P.; Lacôte, E., Electron Paramagnetic Resonance and Computational Studies of Radicals Derived from Boron-Substituted N-Heterocyclic Carbene Boranes. *J. Am. Chem. Soc.* **2011**, *133*, 10312-10321; (b) Walton, J. C.; Makhlof Brahmi, M.; Fensterbank, L.; Lacôte, E.; Malacria, M.; Chu, Q.; Ueng, S.-H.; Solovyev, A.; Curran, D. P., EPR Studies of the Generation, Structure, and Reactivity of N-Heterocyclic Carbene Borane Radicals. *J. Am. Chem. Soc.* **2010**, *132*, 2350-2358; (c) Walton, J. C., Linking Borane with N-Heterocyclic Carbenes: Effective Hydrogen-Atom Donors for Radical Reactions. *Angew. Chem. Int. Ed.* **2009**, *48*, 1726-1728. (d) Ueng, S.-H.; Solovyev, A.; Yuan, X.; Geib, S. J.; Fensterbank, L.; Lacôte, E.; Malacria, M.; Newcomb, M.; Walton, J. C.; Curran, D. P., N-Heterocyclic Carbene Boryl Radicals: A New Class of Boron-Centered Radical. *J. Am. Chem. Soc.* **2009**, *131*, 11256-11262.

5. Dai, W.; McFadden, T. R.; Curran, D. P.; Fruchtl, H. A.; Walton, J. C., 5-*Endo* Cyclizations of NHC-Boraallyl Radicals Bearing Ester Substituents. Characterization of Derived 1,2-Oxaborole Radicals and Boralactones. *J. Am. Chem. Soc.* **2018**, *140*, 15868-15875.

6. T. R. McFadden, C. Fang, S. J. Geib, E. Merling, P. Liu, D. P. Curran, Synthesis of Boriranes by Double Hydroboration Reactions of N-Heterocyclic Carbene Boranes and Dimethyl Acetylenedicarboxylate, *J. Am. Chem. Soc.* **2017**, *139*, 1726-1729.

7. DeGroot, M. S.; Lamb, J., Ultrasonic Relaxation in the Study of Rotational Isomers, *Proc. R. Soc. London, Ser. A* **1957**, *242*, 36-56.

8. Cherniak, E. A.; Costain, C. C., Microwave Spectrum and Molecular Structure of *trans*-Acrolein. *J. Chem. Phys.* **1966**, *45*, 104-110.

9. Bolton, K.; Lister, D. G.; Sheridan, J., Rotational Isomerism, Barrier to Internal Rotation and Electric Dipole Moment of Acrylic Acid by Microwave Spectroscopy. *J. Chem. Soc., Faraday Trans. 2* **1974**, *70*, 113-123.

10. Lung-min, W.; Fischer, H., Electron Spin Resonance of Alpha-(Alkoxycarbonyl)Alkyl Radicals in Solution. *Helv. Chim. Acta*, **1983**, *66*, 138-147.

11. Strub, W.; Roduner, E.; Fischer, H., Isomerization Kinetics of Partly Delocalized Radicals Observed by Muon Spin Rotation. *J. Phys. Chem.* **1987**, *91*, 4379-4383.

12. Newcomb, M.; Horner, J. H.; Filipkowski, M. A.; Ha, C.; Park, S. U., Absolute Rate Constants for Reactions of Alpha-Carbethoxy and Alpha-Cyano Radicals. *J. Am. Chem. Soc.* **1995**, *117*, 3674-3684.

13. Korth, H.-G.; Trill, H.; Sustmann, R., [1-²H]-Allyl Radical. Barrier to Rotation and Allyl Delocalization Energy. *J. Am. Chem. Soc.* **1981**, *103*, 4483-4489.

14. This spectrum was obtained somewhat fortuitously when we conducted an experiment with **3d** in *t*-butylbenzene with 5% allyl bromide to see if we could intercept the boraallyl radical by bromine atom abstraction prior to cyclization. This reaction did not occur, and instead we obtained a high quality 2nd derivative spectrum of the oxaborole radical, which evidently did not react with allyl bromide either.

15. (a) Baguley, P. A.; Walton, J. C., Flight from the Tyranny of Tin: The Quest for Practical Radical Sources Free from Metal Encumbrances. *Angew. Chem., Int. Ed. Eng.* **1998**, *37*, 3072-

3082; (b) Studer, A.; Amrein, S., Tin Hydride Substitutes in Reductive Radical Chain Reactions.

Synthesis **2002**, 835-849.

16. Pan, X.; Lalevée, J.; Lacôte, E.; Curran, D. P., Disulfides and Boryl Sulfides Serve as Both Initiators and Precatalysts in Radical Reductions of Halides by an N-Heterocyclic Carbene Borane. *Adv. Synth. Catal.* **2013**, 355, 3522-3526.

17. Sucrow, W.; Lübbe, F., Acetylenedicarbonsäure-di-*tert*-butylester Und Seine Cyclotrimerisierung. *Angew. Chem.* **1979**, 91, 157-158.

Table of Contents Graphic

